Solvability of Geometric Integrators for Multi-body Systems

Marin Kobilarov

January 6, 2014

Abstract

   This paper is concerned with the solvability of implicit time-stepping methods for simulating the dynamics of multi-body systems. The standard approach is to select a time-step based on desired level of accuracy and computational efficiency of integration. Implicit methods impose an additional but often overlooked requirement that the resulting nonlinear root-finding problem is solvable and has a unique solution. Motivated by empirically observed integrator failures when using large time-steps this work develops bounds on the chosen time-step which guarantee convergence of the root-finding problem solved with Newton's method. Second-order geometric variational integrators are used as a basis for the numerical scheme due to their favorable numerical behavior. In addition to developing solvability conditions for systems described by local coordinates, this work initiates a similar discussion for Lie group integrators which are a favored choice for floating-base systems such as robotic vehicles or molecular structures.

1   Introduction

This work considers the solvability of implicit low-order numerical integrators for multi-body systems with respect to the choice of integration time-step. Our main focus is on geometric variational integrators [1, 15], i.e. integrators which by construction preserve the following physical invariants of the continuous system: symmetries due to conservation laws and associated momentum evolution, configuration space structure such as arising in freely rotating rigid bodies, symplectic phase-space structure. Integrators that respect such variational properties exhibit improved numerics and remedy many practical issues in physically based simulation and animation [2]. In addition, they provide good energy conservation over exponentially long simulation times for non-dissipative systems. When non-conservative forces are present, symplectic structure preservation results in a much-improved treatment of damping that is essentially independent of time step [3]. Our focus on such integrators is also motivated by their successful application to multibody systems [4, 5, 6, 7, 8, 9, 10].

   Variational integrators could therefore be used as a basis for developing *computationally efficient* algorithms by choosing large time-steps while still retaining desired accuracy. A standard approach is to select the time-step to achieve a desired local or global integration error (e.g. see [11, 12, 13] in the context of variational integrators and [14] for the general setting of implicit method). But there is also another key condition that must be satisfied, i.e. the algorithmic solvability of the resulting integrator. This is a key issue since almost all variational time-stepping methods for nonlinear systems are implicit and require the solution of potentially complex nonlinear equations. To the author's knowledge, the issue of implicit integrator *solvability* and its connection to time-step selection has not received enough attention despite the wide use of error-based adaptive time-step selection methods. This turns out to be in fact a central issue for gaining efficiency since, as we show, the success of the numerical root-finding method depends on enforcing *strict bounds on the chosen time-step*. To illustrate this point, consider Figure 1 showing the integration of a simple three-link multi-body system using a symplectic forward Euler method [15]. Based on this empirical evidence there is a clear threshold of the chosen time-step h somewhere in the range $h \in (0.125, 0.5)$ seconds above which the integrator always fails due to divergence of the employed Newton's method. This upper bound could become much lower and thus impose stricter time-step limits as the system increases in complexity.

   The main goal if this paper is therefore to obtain formal bounds on the chosen time-steps h to guarantee solvability of the implicit integrator update. Presently, we obtain such bounds for multi-body systems

evolving in a generalized coordinate space $Q = \mathbb{R}^n$ (as described in Section 4) that *are not* subject to unilateral constraints, e.g. from intermittent contacts or collisions. The second goal of the paper is to extend those methods to geometric Lie group integrators for floating-base systems with configuration space $Q = SE(3) \times \mathbb{R}^m$, where $m = n - 6$ denotes the number of internal degrees of freedom from movable joints (Section 5). A number of methods have been developed to take advantage of the differential-geometric and Lie group structure naturally present in multi-body dynamics for numerical integration purposes [16, 17, 18, 19]. For our purposes, we are interested in a coordinate-invariant treatment of evolution in the Euclidean group $SE(3)$ to avoid singularities and associated time-step restrictions as well chart switching necessary with coordinates such as Euler angles. The resulting algorithms exhibit surprisingly accurate numerical behavior even at large time-steps. The convergence properties developed for coordinate spaces do not directly apply to Lie groups and need to be considered in a more extensive study. Initial observations for the simplest case of a single rigid body and encouraging results related to time-step regularity conditions are presented in Section 3.

2   Background on variational Integrators

A mechanical integrator advances a dynamical system forward in time. Such numerical algorithms are typically constructed by directly discretizing the differential equations that describe the trajectory of the system, resulting in an *update rule* to compute the next state in time. In contrast, variational integrators [1] are based on the idea that the update rule for a discrete mechanical system (i.e., the time stepping scheme) should be derived *directly* from a variational principle rather than from the resulting differential equations. This concept of using a unifying principle from which the equations of motion follow (typically through the calculus of variations [20]) has been favored for decades in physics. Chief among the variational principles of mechanics is *Lagrange D'Alembert's principle* which states that the path $q(t)$ (with endpoint $q(t_0)$ and $q(t_1)$) taken by a mechanical system subject to forces $f(t)$ satisfies the *virtual work* principle $\delta \int_{t_0}^{t_1} L(q, \dot{q}) dt + \int_{t_0}^{t_1} f(t) \delta q(t) = 0$, i.e., the state variables $(q, \dot{q})$ evolve such that any variation of the time integral of the *Lagrangian* L of the system (equal to the kinetic minus potential energy) must result from the work done by the force f.

Practically speaking, variational integrators based on Lagrange D'Alembert's principle first approximate the time integral of the continuous Lagrangian and the integral of forces by a *quadrature* rule. This is accomplished using a "discrete Lagrangian," which is a function of two consecutive states q_k and q_{k+1} (corresponding to time t_k and t_{k+1}, respectively):

$$L_d(q_k, q_{k+1}) \approx \int_{t_k}^{t_{k+1}} L(q(t), \dot{q}(t)) dt.$$

and "discrete forces" f_d according to

$$f_d^-(q_k, q_{k+1}, u_k, u_{k+1}) \delta q_k + f_d^+(q_k, q_{k+1}, u_k, u_{k+1}) \delta q_{k+1} \approx \int_{t_k}^{t_{k+1}} f(q(t), \dot{q}(t), u(t)) \delta q(t),$$

where the function $f(q, \dot{q}, u)$ defines generalized forces including control inputs u acting on the system and the discrete *left* and *right* forces f_d^- and f_d^+, respectively, approximate the virtual work on the left (resp. right) section of the interval $[t_k, t_{k+1}]$. A discrete variational principle can now be formulated over the whole path $\{q_0, ..., q_N\}$ and control inputs $\{u_0, \ldots, u_N\}$ defined by the successive position at times $t_k = kh$. This discrete principle requires that

$$\delta \sum_{k=0}^{N-1} L_d(q_k, q_{k+1}) + \sum_{k=0}^{N-1} [f_d^-(q_k, q_{k+1}, u_k, u_{k+1}) \delta q_k + f_d^+(q_k, q_{k+1}, u_k, u_{k+1}) \delta q_{k+1}] = 0, \tag{1}$$

where variations are taken with respect to each position q_k along the path. Thus, if we use D_i to denote the partial derivative w.r.t the ith variable, we must have

$$D_2 L_d(q_{k-1}, q_k) + D_1 L_d(q_k, q_{k+1}) + f_d^+(q_{k-1}, q_k, u_{k-1}, u_k) + f_d^-(q_k, q_{k+1}, u_k, u_{k+1}) = 0 \tag{2}$$

for every three consecutive positions q_{k-1}, q_k, q_{k+1} of the mechanical system. The relationship (2) is known as the *discrete Euler-Lagrange (DEL) equation* and *defines* an integration scheme which computes q_{k+1} using the two previous positions q_k and q_{k-1} and given forces u_{k-1}, u_k, u_{k+1}.
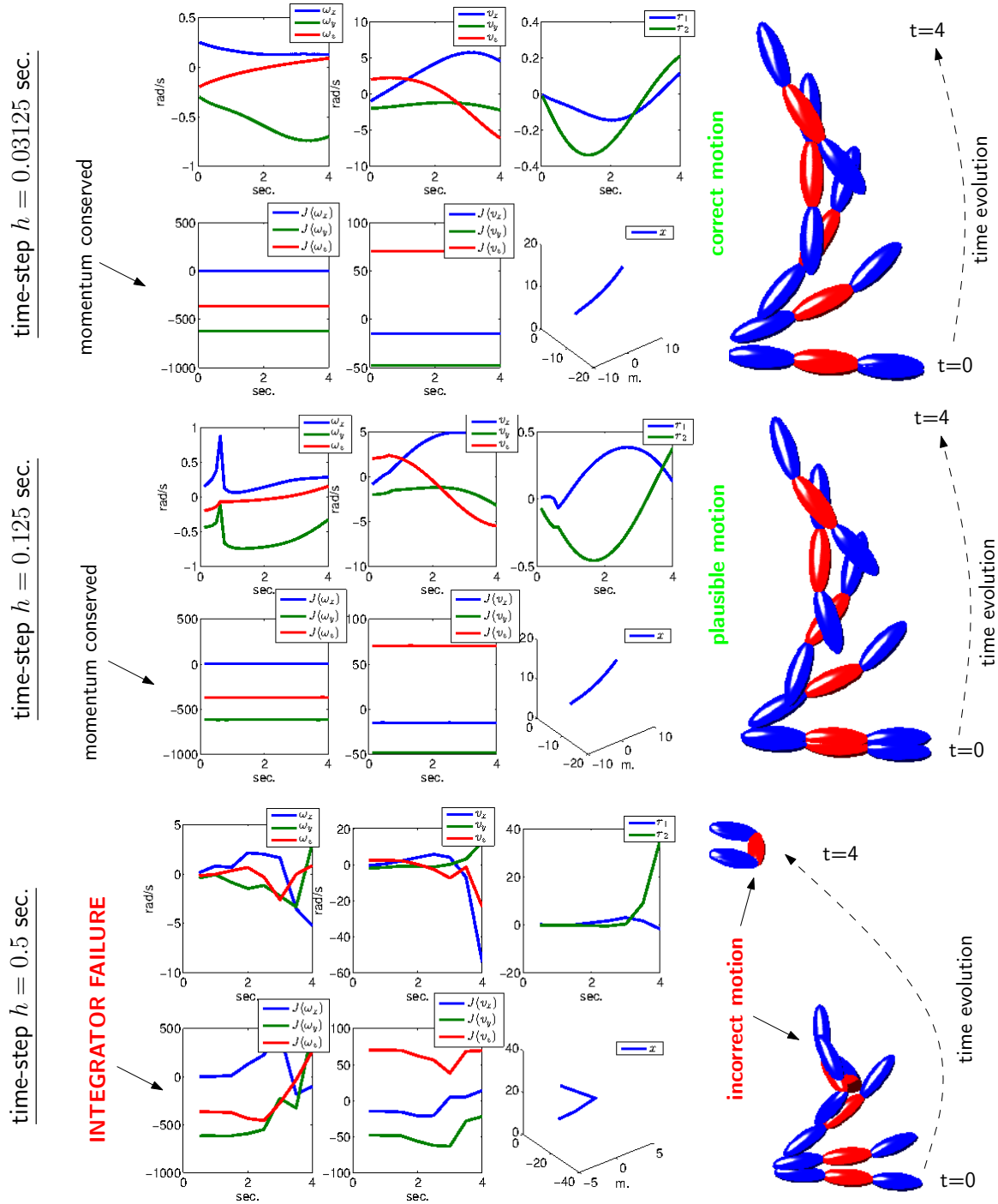
Figure 1: Simulation of a conservative three-link system at three different time-steps. The simulation is qualitatively correct for all time steps below $h = 0.125$ seconds but suddenly breaks down at higher time-steps. It turns out that this is caused either by crossing singular points of the implicit integrator Jacobian or by divergence of the employed Newton's method. This work seeks a priori conditions based on the dynamical model to find bounds on h avoiding such problems.

3

Simple Example. Consider a system with continuous, typical Lagrangian of the form $L(q, \dot{q}) = \frac{1}{2}\dot{q}^T M \dot{q} - V(q)$ (V being a potential function) and subject to control forces only, i.e. $f(q, \dot{q}, u) = u$. Define the discrete Lagrangian using the trapezoidal rule

$$L_d(q_k, q_{k+1}) = \frac{h}{2}\left[L\left(q_k, \frac{q_{k+1} - q_k}{h}\right) + L\left(q_{k+1}, \frac{q_{k+1} - q_k}{h}\right)\right].$$

with discrete forces defined by

$$f_d^-(q_k, q_{k+1}, u_k, u_{k+1}) = \frac{h}{2}u_k, \qquad f_d^+(q_k, q_{k+1}, u_k, u_{k+1}) = \frac{h}{2}u_{k+1}$$

The resulting update equation is:

$$M\frac{q_{k+1} - 2q_k + q_{k-1}}{h^2} = u_k - \nabla V(q_k),$$

which is a discrete analog of Newton's law $M\ddot{q} = u - \nabla V(q)$. This example can be easily generalized to systems with configuration-dependent mass matrix $M(q)$ or to systems with constraints leading to variants of the update equation.

3 Geometric integrators for the rigid body

We first consider geometric integrators for a single rigid body as one of the simplest mechanical system with nonlinear dynamics. The goal is to illustrate two typical geometric integrators and discuss regularity conditions required for their solvability. These results will then be generalized to multi-body systems.

The standard continuous equations of motion of a controlled rigid body is given by (see e.g. [21])

$$\dot{R} = R\hat{\omega} \tag{3}$$

$$\mathbb{J}\dot{\omega} = \mathbb{J}\omega \times \omega + u, \tag{4}$$

where $R \in SO(3)$ is the rotation matrix, $\omega \in \mathbb{R}^3$ is the angular velocity, $\mathbb{J}$ is the 3x3 inertia tensor and u are the given control inputs. While it is possible to express the body rotation using coordinates such as Euler angles a more numerically convenient approach is to perform numerical integration on the configuration manifold directly. For instance, the simplest first-order *Euler method* on $SO(3)$ would take the form

$$R_{k+1} = R_k \exp(h\omega_{k+1}), \tag{5}$$

$$\omega_{k+1} = \omega_k + h\mathbb{J}^{-1}(\mathbb{J}\omega_k \times \omega_k + u_k), \tag{6}$$

where $\exp : \mathbb{R}^3 \to SO(3)$ is the exponential map defined by

$$\exp(\omega) = \begin{cases} I, & \omega = 0 \\ I + \frac{\sin\|\omega\|}{\|\omega\|}\hat{\omega} + \frac{1-\cos\|\omega\|}{\|\omega\|^2}\hat{\omega}^2, & \omega \neq 0 \end{cases}, \tag{7}$$

with I denoting the identity matrix and the map $\hat{\cdot} : \mathbb{R}^3 \to \mathfrak{so}(3)$ (with $\mathfrak{so}(3)$ begin the space of 3x3 skew-symmetric matrices) defined by

$$\hat{\omega} = \begin{bmatrix} 0 & -w_3 & w_3 \\ w_3 & 0 & -w_1 \\ -w_2 & w_1 & 0 \end{bmatrix}. \tag{8}$$

The integrator (5)–(6) explicitly updates the next state (R_{k+1}, ω_{k+1}) given the current state (R_k, ω_k). The method is more accurate than a coordinate-based Euler method and does not require coordinate chart switching [22]. Nevertheless, similarly to any other Euler method it is only first-order accurate and has poor numerical stability which becomes especially pronounced at large time-steps h.

3.1 Implicit second-order methods

A numerically superior integrator results from implicit second-order formulation, for instance based on trapezoidal or midpoint collocation. As an example, a *trapezoidal collocation* of the dynamics (4) will result in the semi-explicit integrator

$$R_{k+1} = R_k \exp(h\omega_{k+1}), \tag{9}$$

$$\mathbb{J}(\omega_{k+1} - \omega_k) = \frac{h}{2} \left(\mathbb{J}\omega_k \times \omega_k + \mathbb{J}\omega_{k+1} \times \omega_{k+1} \right) + hu_k, \tag{10}$$

known as the *trapezoidal Lie-Newmark* (TLN) integrator [15, 23]. The dynamics update (10) can be equivalently written as

$$A(h\omega_{k+1})^T \mathbb{J}\omega_{k+1} - A(-h\omega_k)^T \mathbb{J}\omega_k = hu_k$$

where the matrix $A(\omega)$ is defined by

$$A(\omega) = I - \frac{1}{2}\widehat{\omega},$$

and is regarded as the truncated (to first-order) right-trivialized derivative inverse [23, 24] of the exponential map, i.e. $\operatorname{dexp}(w)^{-1} = A(\omega) + O(\|w\|^2)$. In contrast, a very similar method employing the *untruncated* derivative is actually a variational symplectic integrator obtained using a Lie group version of the discrete variational principle (1) known as the discrete Euler-Poincare principle (see [1, 25, 26, 23, 27]).

An example of such a symplectic Lie group integrator known for its efficiency and ease of implementation [23, 27] is defined by

$$R_{k+1} = R_k \operatorname{cay}(h\omega_{k+1}), \tag{11}$$

$$[\operatorname{dcay}_{h\omega_{k+1}}^{-1}]^T \mathbb{J}\omega_{k+1} - [\operatorname{dcay}_{-h\omega_k}^{-1}]^T \mathbb{J}\omega_k = hu_k, \tag{12}$$

where the Cayley map $\operatorname{cay} : \mathbb{R}^3 \to SO(3)$ approximates the exponential map and is defined by

$$\operatorname{cay}(\omega) = I + \frac{4}{4 + \|\omega\|^2} \left(\widehat{\omega} + \frac{\widehat{\omega}^2}{2} \right), \tag{13}$$

while the right-trivialized tangent inverse is defined by

$$[\operatorname{dcay}_\omega^{-1}] = I - \frac{\widehat{\omega}}{2} + \frac{\omega\omega^T}{4}. \tag{14}$$

One of the special properties of the symplectic integrator (11)-(12) is that it preserves the spatial momentum $J_k \approx J(kh)$ given by $J_k = R_k [\operatorname{dcay}_{-h\omega_k}^{-1}]^T \mathbb{J}\omega_k$ in the absence of forces, i.e. when $u_k = 0$.

Time-step selection and solvability. The numerical behavior, preservation properties, and associated backward error analysis of these methods has been established [28, 22, 15, 23, 2]. The resulting favorable numerical behavior permits the use of larger time-steps h while maintaining desired accuracy and stability. But how large can h be? To answer this question we next study regularity conditions of the most common iterative method, i.e. Newton's method, which translate to a maximum time-step selection rule required in order to guarantee solvability of the integrators.

3.2 Newton's method and time-step bounds

Either the collocation or the symplectic methods require the solution of nonlinear discrete dynamics equations, in particular equations (10) or (12), respectively. This can be formulated as the solution of the nonlinear equations $e_{\text{tln}}(\omega_{k+1}) = 0$ or $e_{\text{symp}}(\omega_{k+1}) = 0$ given by

$$e_{\text{tln}}(\omega) = \left[I + \frac{h}{2}\widehat{\omega} \right] \mathbb{J}\omega - c_k, \tag{15}$$

where $c_k \in \mathbb{R}^3$ is given and defined by

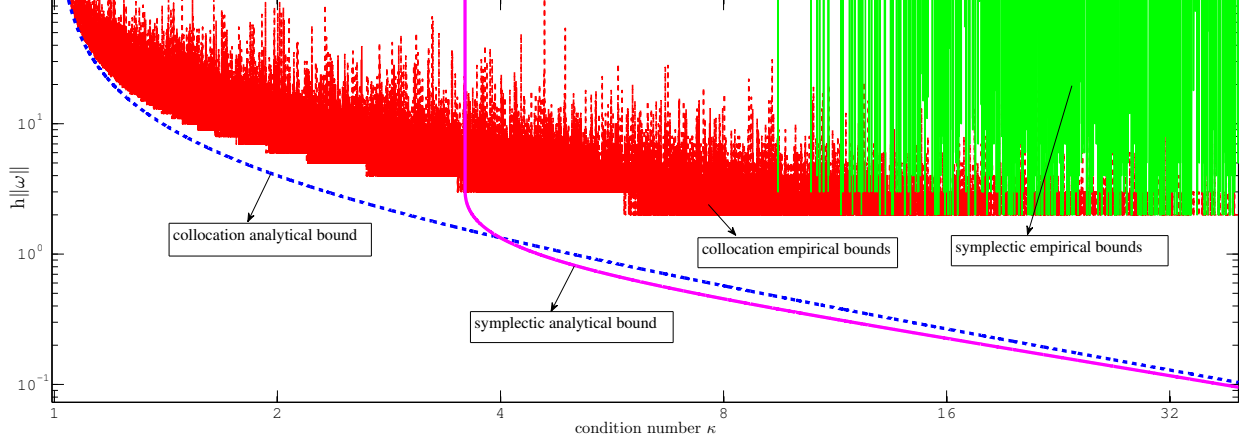$$c_k = A(-h\omega_k)^T \mathbb{J}\omega_k + hu_k,$$

5

Figure 2: Comparison of maximum time-steps h allowed by the trapezoidal collocation integrator and the symplectic integrator. Both analytical upper bounds are shown as well as empirically computed upper bounds resulting in singular Jacobians (and integrator solution failure) from 50000 Monte Carlo experiments with varying inertia $\mathbb{J}$ and velocity ω.

and

$$e_{\mathrm{symp}}(\omega) = \left[I + \frac{h}{2}\widehat{\omega} + \frac{h^2}{4}\omega\omega^T \right] \mathbb{J}\omega - d_k, \tag{16}$$

where $d_k \in \mathbb{R}^3$ is given and defined by

$$d_k = [\mathrm{dcay}_{-h\omega_k}^{-1}]^T \mathbb{J}\omega_k + hu_k.$$

While it is possible to apply a number of numerical root-finding methods including polynomial and continuation methods, we focus on Newton-like methods since they generalize to the more complex multi-body setting. Newton's method solves the equation $e(\omega) = 0$ using an initial guess ω which is then iterated according to $w = w - [De(w)]^{-1}e(\omega)$, where $De(\omega)$ is the Jacobian of $e(\omega)$ which must be invertible. The Jacobians of the two methods are given by

$$De_{\mathrm{tln}}(\omega) = \mathbb{J} - \frac{h}{2}\widehat{\mathbb{J}\omega} + \frac{h}{2}\widehat{\omega}\mathbb{J}, \tag{17}$$

and

$$De_{\mathrm{symp}}(\omega) = \mathbb{J} - \frac{h}{2}\widehat{\mathbb{J}\omega} + \frac{h}{2}\widehat{\omega}\mathbb{J} + \frac{h}{4}\omega^T\mathbb{J}\omega I + \frac{h}{2}\omega\omega^T\mathbb{J}, \tag{18}$$

and are positive definite and invertible at $h = 0$. We next compute the range of time-steps h for which the Jacobians remain invertible. First note that it is not difficult to show [1] that

$$\widehat{\omega}\mathbb{J} \leqslant \frac{1}{2}\|\omega\|(\sigma_+ - \sigma_-)I,$$

where σ_- and σ_+ are the minimum and maximum eigenvalues of $\mathbb{J}$. Therefore, we have

$$De_{\mathrm{tln}}(\omega) \geqslant \left[\sigma_- - \frac{h}{4}\|\omega\|(\sigma_+ - \sigma_-) \right] I,$$

or equivalently $De_{\mathrm{tln}}(\omega)$ will be always positive definite and hence invertible if the time-step is chosen according to $0 < h < \bar{h}_{\mathrm{tln}}(\omega)$ where the upper bound is defined by

$$\bar{h}_{\mathrm{tln}}(\omega) = \begin{cases} \infty \ \ (\text{i.e. time-step unrestricted}) & \text{if either } \kappa = 1, \text{ or } \|\omega\| = 0 \\ \frac{4}{(\kappa-1)\|\omega\|} & \text{otherwise}, \end{cases} \tag{19}$$

---

[1] $A \geqslant B$ for any matrices $A, B \in \mathbb{R}^{n \times n}$ if and only if $x^T A x \geqslant x^T B x$ for all $x \in \mathbb{R}^n$.

where $\kappa = \frac{\sigma_+}{\sigma_-} \geqslant 1$ is the *condition number* of $\mathbb{J}$. When $\kappa = 1$ (i.e. a spherical body) or when $\|\omega\| = 0$ we have trivially $De_{\text{tln}} = \mathbb{J}$ and there are no restrictions on the time-step.

The symplectic integrator Jacobian $De_{\text{symp}}(\omega)$ satisfies

$$De_{\text{symp}}(\omega) \geqslant \left[\sigma_- - \frac{h}{4} \|\omega\| (\sigma_+ - \sigma_-) + h^2 \|\omega\|^2 \left(\sigma_- - \frac{1}{4}\sigma_+ \right) \right] I,$$

and will remain positive definite and invertible all time-steps $0 \leqslant h < \bar{h}_{\text{symp}}(\omega)$ where the upper bound is defined by

$$\bar{h}_{\text{symp}}(\omega) = \begin{cases} \infty \quad (\text{ i.e. time-step unrestricted}) & \text{if either } \kappa \leqslant 4\sqrt{7} - 7, \text{ or } \|\omega\| = 0 \\ \frac{\kappa - 1 - \sqrt{\kappa^2 + 14\kappa - 63}}{(8 - 2\kappa)\|\omega\|} & \text{otherwise.} \end{cases} \tag{20}$$

Figure 2 illustrates these bounds by plotting the dependence of $h\|\omega\|$ on the condition number κ. The key point is that the lower the condition number and the lower the velocity magnitude $\|\omega\|$ the higher time-step can be chosen. Note that the symplectic integrator appears to have a wider region of convergence and, unlike collocation, there are no restrictions on the maximum time-step for bodies with condition number $\kappa \approx 3.58$ or smaller. Furthermore, empirically the number of failed solutions is a small fraction of the singular cases for the collocation scheme. In general, though both methods are suitable for very efficient and long-term stable integration as long as the time-step h is chosen to satisfy the respective bounds (19) or (20).

4 Variational integrators for mechanical systems in generalized coordinates

We next consider the more general setting of mechanical systems in minimal generalized coordinates, i.e. describing the the system joint angles and pose. The equations of motion of multi-body systems can be derived using a Lagrangian in the typical form

$$L(q, \dot{q}) = \frac{1}{2} \dot{q}^T M(q) \dot{q} - V(q),$$

where $M(q)$ is a positive-definite mass matrix and V is a potential function. The system is also subject to generalized forces $f(q, \dot{q}, u)$ in the form

$$f(q, \dot{q}, u) = f^x(q, \dot{q}) + B(q)u,$$

where f^x encodes any internal and external forces e.g. due to damping or friction and $u \in \mathbb{R}^c$ are the control forces. Our focus is on second-order variational integrators obtained using the discrete Lagrangian

$$L_d(q_k, q_{k+1}) = \frac{h}{2} \left[L(q_k, v_{k+1}) + L(q_{k+1}, v_{k+1}) \right],$$

where the discrete velocity $v_k \in \mathbb{R}^n$ is defined by

$$v_k \triangleq \frac{q_k - q_{k-1}}{h},$$

and discrete forces set to

$$f_d^-(q_k, q_{k+1}, u_k, u_{k+1}) = \frac{h}{2} f(q_k, v_{k+1}, u_k), \qquad f_d^+(q_k, q_{k+1}, u_k, u_{k+1}) = \frac{h}{2} f(q_{k+1}, v_{k+1}, u_{k+1}).$$

This choice of discretization is based on trapezoidal quadrature approximation and as we will show results in a simpler integrator amenable to easier analysis compared to other methods of the same order such as midpoint quadrature (that is not to say that the midpoint rule is inferior).

Discrete Equations of Motion. The general discrete Euler-Lagrange equations (2) when applied to the mechanical systems result in the implicit integrator

$$\frac{1}{2}[M(q_k) + M(q_{k+1})]v_{k+1} - \frac{1}{2}[M(q_{k-1}) + M(q_k)]v_k$$
$$- \frac{h}{4}\left[(I_n \otimes v_k^T)\nabla M(q_k)v_k + (I_n \otimes v_{k+1}^T)\nabla M(q_k)v_{k+1}\right] + h\nabla V(q_k) \qquad (21)$$
$$= \frac{h}{2}[f(q_k, v_k, u_k) + f(q_k, v_{k+1}, u_k)]$$

where the tensor product notation $A \otimes B$ is defined (see e.g. [29]) according to

$$A \otimes B = \begin{bmatrix} a_{11}B & \cdots & a_{1n}B \\ \vdots & \ddots & \vdots \\ a_{n1}B & \cdots & a_{nn}B \end{bmatrix}$$

and the matrix gradient ∇M and hence the expression $(I_n \otimes v^T)\nabla M$ are defined as

$$\nabla M = \begin{bmatrix} \frac{\partial M}{\partial q_1} \\ \vdots \\ \frac{\partial M}{\partial q_n} \end{bmatrix}, \qquad (I_n \otimes v^T)\nabla M = \begin{bmatrix} v^T\frac{\partial M}{\partial q_1} \\ \vdots \\ v^T\frac{\partial M}{\partial q_n} \end{bmatrix}.$$

Equivalently, the matrix $(I_n \otimes v^T)\nabla M$ can be expressed in coordinates according to

$$[(I_n \otimes v^T)\nabla M]_{ij} \triangleq \sum_{\ell=1}^{n} \frac{\partial M_{\ell j}}{\partial q_i} v_\ell,$$

where $i, j = 1, \ldots, n$ are the matrix row and column indices, respectively. The relationship (21) is expressed more compactly as

$$\frac{1}{2}[M(q_k) + M(q_k + hv_{k+1})]v_{k+1} - \frac{1}{2}[M(q_{k-1}) + M(q_k)]v_k + hb_k(v_k, q_k, v_{k+1}) = hB(q_k)u_k, \qquad (22)$$

where the *discrete bias* b_k is defined by

$$b_k(v_k, q_k, v_{k+1}) = -\frac{1}{4}\left[(I_n \otimes v_k^T)\nabla M(q_k)v_k + (I_n \otimes v_{k+1}^T)\nabla M(q_k)v_{k+1}\right] + \nabla V(q_k)$$
$$- \frac{1}{2}[f^x(q_k, v_k) + f^x(q_k, v_{k+1})]. \qquad (23)$$

The integrator (22) can be regarded as the discrete analog of the continuous equations of motion in a standard form (e.g. [30, 31])

$$M(q)\ddot{q} + b(q, \dot{q}) = B(q)u,$$

where the corresponding *continuous bias* term $b(q, \dot{q}) = C(q, \dot{q})\dot{q} + g(q) - f^x(q, \dot{q})$ encodes Coriolis and centripetal forces defined by the matrix C, gravity forces g, and other forces f^x.

4.1 Implicit time-stepping using a Newton algorithm

The integrator (21) is solved in terms of the next velocity v_{k+1} using a numerical root-finding procedure, typically a second-order method such as Newton's method equipped with regularization and line-search procedures. Our goal is to find the root of the equation $e_k(v_{k+1}) = 0$ corresponding to the relationship (21) with the mapping $e_k : \mathbb{R}^n \to \mathbb{R}^n$ defined by

$$e_k(v) \triangleq \frac{1}{2}[M(q_k) + M(q_k + hv)]v - \frac{1}{2}[M(q_{k-1}) + M(q_k)]v_k + h[b_k(v_k, q_k, v) - B(q_k)u_k]. \qquad (24)$$

The Jacobian of $e_k(v)$ is

$$De_k(v) = \frac{1}{2}[M(q_k) + M(q_k + hv)] + \frac{h}{2}\left[\nabla M(q_k + hv)^T(I \otimes v) - (I \otimes v^T)\nabla M(q_k) - D_2 f^x(q_k, v)\right], \quad (25)$$

8

where the matrix gradient transpose paired with the tensor product should be understood as

$$\nabla M^T (I \otimes v) \equiv \left[\begin{array}{cccc} \frac{\partial M^T}{\partial q_1} v, & \cdots & , \frac{\partial M^T}{\partial q_n} v \end{array} \right].$$

Note that one of the main practical advantages of using a trapezoidal variational formulation, in addition to its numerical stability, is the relatively simple expression for the Jacobian (25). This is not the case if the midpoint rule were used which would involve the unwieldy term $\nabla^2 M$.

Newton's algorithm starts by setting the unknown v to an initial value and iteratively updates it to $v + d$ where the Newton step d is defined by

$$d = -De_k(v)^{-1} e_k(v).$$

We will restrict our analysis to this "pure" version of the algorithm which also employs the previous velocity as an initial value, i.e. the first iteration begins with $v = v_k$. The algorithm is summarized below.

Algorithm 1: $v_{k+1} \leftarrow \texttt{Newton}\,(v_k, q_k, u_k)$

---
1 $v \leftarrow v_k$
2 choose time-step h
3 **while** v *has not converged* **do**
  | Compute $d \in \mathbb{R}^n$ such that $[De_k(v)]d = -e_k(v)$ using (24) and (25)
  | $v \leftarrow v + d$
4 return v

We next study the convergence properties of this algorithm. This will be accomplished by assuming certain regularity conditions of the dynamical model and deriving time-step bounds to guarantee convergence.

4.2 Convergence of Newton's method

In order to guarantee solvability of the integrator it is critical to ensure that the time-step h is chosen small enough to ensure convergence of Algorithm (1) or in other words that the true solution can be traced from the initial guess $v = v_k$. This problem has been studied previously [32] for implicit time-stepping methods under general regularity conditions. For mechanical multi-body systems these results need to be extended since it turns out that the Jacobian Lipschitz "constant" normally employed in the Kantorovich-type results [32] is actually a function of the time-step and the current state which requires additional development.

To establish the formal bounds it is necessary to assume the following regularity conditions of the dynamical model:

Assumption 1. *Assume that the dynamical system model satisfies the following bounds:*

$$m_1(q)I \leqslant M(q) \leqslant I m_2(q) \tag{26}$$

$$\|M(q) - M(q+w)\| \leqslant \ell_0(q)\|w\| \tag{27}$$

$$\|\nabla M(q)^T (I_n \otimes v)\| \leqslant \ell_1(q)\|v\| \tag{28}$$

$$\left\| [\nabla M(q+w) - \nabla M(q)]^T (I_n \otimes v) \right\| \leqslant \ell_2(q)\|v\|\|w\| \tag{29}$$

$$\|D_2 f^x(q,v)\| \leqslant \ell_3(q)\|v\| + \ell_4(q) \tag{30}$$

$$\|D_2 f^x(q,v) - D_2 f^x(q,v+d)\| \leqslant [\ell_5(q)\|v\| + \ell_6(q)]\|d\| \tag{31}$$

for some known non-negative functions $m_1, m_2, \ell_0, \ell_1, \ldots, \ell_6 : Q \to \mathbb{R}_{\geqslant 0}$ for any $v, w, d \in \mathbb{R}^n$. Furthermore, assume that there is a set $U \subset Q$ and constants $\bar{m}_1, \bar{m}_2, \bar{\ell}_0, \ldots, \bar{\ell}_6 \geqslant 0$ such that for all $q \in U$:

$$\bar{m}_1 \leqslant m_1(q), \quad m_2(q) \leqslant \bar{m}_2, \quad \ell_0(q) \leqslant \bar{\ell}_0 \quad, \ldots, \quad \ell_6(q) \leqslant \bar{\ell}_6.$$

The bounds defined in (26)–(31) are used to obtain regularity conditions which are necessary to guarantee convergence of Newton's method. In particular, the following quantities will be computed in order to construct a convergence proof:

- bound on time-step h to guarantee non-singular Jacobian $De_k(v)$ for a given $v \in \mathbb{R}^n$
- bound on $\|e_k(v_k)\|$ and Jacobian inverse $\|De_k(v_k)^{-1}\|$ at first Newton iteration, i.e. when $v = v_k$
- bound on h so that $De_k(v)$ is invertible for all all Newton iterations staring with $v = v_k$
- Lipschitz bound on the Jacobian $De_k(v)$

This list constitute the steps to be taken in order to construct a Kantorovich-type proof of convergence.

4.2.1 Jacobian Regularity.

The most basic requirement for convergence is that the Jacobian De_k defined in (25) is non-singular, a condition established as follows.

Proposition 1. *Assume that the conditions (26)–(31) hold. The Jacobian $De_k(v)$ is non-singular for every time-step h such that $0 \leqslant h < \bar{h}(q_k, v)$ where the upper bound is defined by*

$$\bar{h}(q_k, v) = \frac{\sqrt{[\ell_3(q_k)\|v\| + \ell_4(q_k)]^2 + 8\ell_2(q_k)\|v\|^2 \bar{m}_1} - \ell_3(q_k)\|v\| - \ell_4(q_k)}{2\ell_2(q_k)\|v\|^2} \tag{32}$$

Proof. First, note that at $h = 0$ we have $De_k(v) = M(q_k) > 0$, i.e. the Jacobian is positive definite[2]. Therefore, h can be increased as long as De_k remains positive definite and hence invertible. Next we add and subtract the term $\nabla M^T(I_n \otimes v)$ to De_k in (25) and since the matrix

$$\nabla M^T(I_n \otimes v) - (I_n \otimes v^T)\nabla M$$

is skew-symmetric it will not affect the Jacobian positivity. Hence we have

$$\begin{aligned}
De_k(v) &\geqslant \frac{1}{2}[M(q_k) + M(q_k + hv)] + \frac{h}{2}\left[\nabla M(q + hv)^T(I_n \otimes v) - \nabla M(q)^T(I_n \otimes v) - D_2 f^x(q_k, v)\right] \\
&\geqslant \max\left[m_1(q_k) - \frac{h}{2}\|v\|\ell_0(q_k), \bar{m}_1\right] - \frac{h}{2}\left[\ell_2(q_k)h\|v\|^2 + \ell_3(q_k)\|v\| + \ell_4(q_k)\right],
\end{aligned} \tag{33}$$

where $\max(\cdot, \cdot)$ takes the maximum of either the local bound at q_k or the global bound $\bar{m}_1$ of the mass matrix. For simplicity, we will employ the global bound so that $De_k(v) > 0$ when h is chosen so that

$$\ell_2(q_k)\|v\|^2 h^2 + [\ell_3(q_k)\|v\| + \ell_4(q_k)]h - 2\bar{m}_1 < 0$$

which is satisfied when $h < \bar{h}(q_k, v)$ where $\bar{h}$ is the quadratic equation root defined in (32). Note that in case when $\ell_2(q_k)\|v\| = 0$ we have the simpler form

$$\bar{h}(q_k, v) = \frac{2\bar{m}_1}{\ell_3(q_k)\|v\| + \ell_4(q_k)}.$$

Finally, whenever the denominator is zero there are no restriction on the time-step, i.e. $\bar{h}(q_k, v) = \infty$. $\quad\square$

Linear Damping Forces. Note that the Jacobian regularity bound can be improved when the velocity-dependent terms in the external forces $f^x(q, v)$ are the form $-Kv$ for some matrix $K > 0$. The quadratic condition would then be

$$\ell_2(q_k)\|v\|^2 h^2 + [\ell_4(q_k) - k_1]h - 2\bar{m}_1 < 0,$$

where $k_1 > 0$ is such that $k_1 I \leqslant K$ with respect to the chosen norm $\|\cdot\|$.

---

[2]any matrix (including non-symmetric) $A \in \mathbb{R}^{n \times n}$ is positive definite if $x^T A x > 0$ for all $x \in \mathbb{R}^n$ such that $x \neq 0$

4.2.2 Bounding Newton's method iterates.

Next, we establish bounds on the error function e_k and inverse Jacobian De_k evaluated at the first Newton iteration, i.e. when $v = v_k$. These bound will then be used in computing the the region of convergence of Newton's method determined by the first search step.

Applying the assumption (27) twice the following relationship holds

$$\frac{1}{2}[M(q_k + hv_k) - M(q_k - hv_k)]v_k \leqslant h\ell_0(q_k)\|v_k\|^2,$$

and a bound on the residual e_k evaluated at $v = v_k$ can be established according to

$$\|e_k(v_k)\| \leqslant h\ell_0(q_k)\|v_k\|^2 + h\|b_k(v_k) - B(q_k)u_k\|$$
$$\triangleq hL_0(q_k, v_k). \tag{34}$$

Similarly, the Jacobian satisfies the following bound

$$\|De_k(v_k)\| \leqslant \bar{m}_2 + h\left[\bar{\ell}_1\|v_k\| + \frac{1}{2}\|D_2f(q_k, v_k)\|\right]$$
$$\triangleq \bar{m}_2 + hL_1(q_k, v_k), \tag{35}$$

while its inverse is bounded according to

$$\|De_k(v_k)^{-1}\| \leqslant \frac{1}{\bar{m}_1 - hL_1(q_k, v_k)}. \tag{36}$$

Note that similarly to (33) it is possible to obtain a tighter bound by using $\min\left[m_2(q_k) + \frac{h}{2}\|v_k\|\ell_0(q_k), \bar{m}_2\right]$ in place of $\bar{m}_2$ in (35) and (36) with minimal modification; we employ the simpler $\bar{m}_2$ for clarity.

The first Newton iteration search step $d_0 \in \mathbb{R}^n$ is defined by

$$d_0 \triangleq -[De_k(v_k)]^{-1}e_k(v_k).$$

A convergent Newton algorithm will then perform iterations in the vicinity of the starting value $v = v_k$ in the sense that all iterates v will be contained in the set $\mathcal{B}_0 \triangleq \mathcal{B}(v_k + d_0, \|d_0\|)$, i.e. the ball at point $v_k + d_0$ with radius $\|d_0\|$. More formally, the set $\mathcal{B}(v, r) \subset \mathbb{R}^n$ for a given scalar $r > 0$ is defined as

$$\mathcal{B}(v, r) = \{v + d \mid \|d\| \leqslant r\}.$$

The following property related to the magnitude of subsequent iterates can be established:

Lemma 4.1. *Let assumptions* (26)–(31) *hold and assume that the time-step h is such that $\mathcal{B}_0 \subset U$. All Newton iterates $v \in \mathbb{R}^n$ are then bounded according to*

$$\|v\| \leqslant \|v_k\| + \frac{2hL_0(q_k, v_k)}{\bar{m}_1 - hL_1(q_k, v_k)}. \tag{37}$$

Proof. Assuming the Jacobian $De_k(v)$ is invertible for all $v \in \mathcal{B}_0$, all consequent iterates v will remain inside $\mathcal{B}_0$ which means that

$$\|v\| \leqslant \|v_k + d_0\| + \|d_0\|$$
$$\leqslant \|v_k\| + 2\|d_0\|$$
$$\leqslant \|v_k\| + 2\|De_k(v_k)^{-1}\|\|e_k(v_k)\|,$$

and (37) follows from (34) and (36). □

4.2.3 The Newton-Kantorovich Condition

So far we obtained condition (32) on h guaranteeing that the Jacobian De_k is invertible. The computed upper bound $\bar{h}(q_k, v)$ is a function of v so it is actually not possible to use this bound to guarantee regularity for all Newton iterations a priori, i.e. before executing the algorithm, since obviously v will change at each iteration. But since know that $\|v\|$ is bounded such an a-priori condition is obtained using the upper bound (37) by selecting h so that $\phi_k(h) < 0$ where

$$\phi_k(h) = \ell_2 \left[\|v_k\| + \frac{2hL_0}{\bar{m}_1 - hL_1} \right]^2 h^2 + \left[\ell_3 \cdot \left(\|v_k\| + \frac{2hL_0}{\bar{m}_1 - hL_1} \right) + \ell_4 \right] h - \bar{m}_1, \tag{38}$$

where all functions ℓ_i and L_i are evaluated at (q_k, v_k). This is now a fourth-order polynomial in h and the upper bound denoted by $\bar{h}_k$ is set to the *smallest positive root of* $\phi_k(h)$.

Next, we establish a Lipschitz condition on the Jacobian. We have, for some $d \in \mathbb{R}^n$:

$$
\begin{aligned}
\|De_k(v + d) - De_k(v)\| \leqslant\ & \frac{1}{2} \|M(q_k + h(v + d)) - M(q_k + hv)\| \\
& + \frac{h}{2} \left\| \nabla M \left(q_k + h(v + d) \right)^T (I \otimes (v + d)) - \nabla M(q_k + hv)^T (I \otimes v) \right. \\
& \left. - (I \otimes d^T) \nabla M(q_k) - D_2 f^x(q_k, v + d) + D_2 f^x(q_k, v) \right\| \\
\leqslant\ & \frac{h}{2} \left[\bar{\ell}_0 + 2\bar{\ell}_1 + \bar{\ell}_2 \|v\| + \ell_5(q_k) \|v\| + \ell_6(q_k) \right] \|d\| \\
\triangleq\ & h \left[L_2(q_k) + L_3(q_k) \|v\| \right] \|d\|.
\end{aligned}
\tag{39}
$$

In order to obtain a Lipschitz bound independent of the velocity v it is necessary to employ bound (37) on $\|v\|$ which leads to

$$
\begin{aligned}
\|De_k(v + d) - De_k(v)\| \leqslant\ & h \left[L_2(q_k) + L_3(q_k) \left(\|v_k\| + \frac{2hL_0(q_k, v_k)}{\bar{m}_1 - hL_1(q_k, v_k)} \right) \right] \|d\| \\
=\ & \frac{h[L_2 \bar{m}_1 + L_3 \|v_k\| \bar{m}_1] + h^2 \left[2L_0 L_3 - L_1 L_2 - L_1 L_3 \|v_k\| \right]}{\bar{m}_1 - hL_1} \|d\| \\
\triangleq\ & \frac{hL_4 + h^2 L_5}{\bar{m}_1 - hL_1} \|d\|,
\end{aligned}
\tag{40}
$$

so that the factor in front of $\|d\|$ can now be regarded as the required Lipschitz constant of the Jacobian [32].

Choosing $h < \bar{h}_k$ where $\bar{h}_k$ is the smallest positive root of $\phi_k(h)$ guarantees that the Jacobian is invertible for all Newton iterations assuming the method was initialized with $v = v_k$. This bound can now be combined with the actual sufficient condition for convergence. As a result, a stricter bound will be obtained that is sufficient to guarantee a successful solution.

Proposition 2. *Assume that conditions (26)–(31) hold and that the time-step h is such that $\phi_k(h') < 0$ for all $h' \in [0, h]$ or equivalently assume that $h < \bar{h}_k$. Furthermore, assume that $\mathcal{B}_0 \subset U$ for all $h \leqslant \bar{h}_k$. Newton's algorithm then converges super-linearly to a unique solution inside $\mathcal{B}_0$ if the time-step h is chosen so that $\psi(h') < 0$ for all $h' \in [0, h]$ where*

$$\psi(h) = h^3 (2L_0 L_5 + L_1^3) + h^2 (2L_0 L_4 - 3\bar{m}_1 L_1^2) + h(2\bar{m}_1^2 L_1) - \bar{m}_1^3. \tag{41}$$

Equivalently, convergence is ensured if the upper bound on h is set to the smallest positive root of $\psi(h) = 0$.

Proof. To ensure convergence, the Newton-Kantorovich theorem [33] requires that

$$\frac{hL_4 + h^2 L_5}{\bar{m}_1 - hL_1} \|De_k^{-1}(v_k)\| \|d_0\| \leqslant \frac{1}{2}, \tag{42}$$

where the first term corresponds to the Jacobian Lipschitz term (40). Note that

$$
\begin{aligned}
\|De_k^{-1}(v_k)\| \|d_0\| &\leqslant \|De_k^{-1}(v_k)\|^2 \|e_k(v_k)\| \\
&\leqslant \frac{hL_0(q_k, v_k)}{[\bar{m}_1 - hL_1(q_k, v_k)]^2},
\end{aligned}
$$

12

using the computed bounds (34) and (36), which is then substituted into (42) to obtain $\psi(h) < 0$. Since this condition is trivially satisfied for $h = 0$ the upper bound is the smallest positive h for which $\psi(h) = 0$. $\qquad\square$

5 Variational Lie Group Integrators for Multibody Systems

The integrators developed in Section 4 are based on generalized coordinates q in the Euclidean space $\mathbb{R}^n$. The configuration space Q is actually only locally isomorphic to $\mathbb{R}^n$ in the sense that any choice of rotational coordinates such as Euler angles cannot globally cover the space of rotations using a single chart. Most floating-base multi-body systems have a configuration space $Q = SE(3) \times \mathbb{R}^m$ with $q = (g, r)$ where $g \in SE(3)$ is the pose of a chosen *base body* and $r \in \mathbb{R}^m$ are the joint angles or *shape variables*. Such representation is sufficient for tree-topology multi-body systems with m internal (i.e. from movable joints) degrees of freedom. A more general graph-topology system with loops is modeled by selecting a spanning tree and enforcing loop constraints using additional multiplier variables. Our goal is to develop geometric variational integrators for such systems which evolve intrinsically on the configuration space Q. These integrators can be regarded as an extension of the single rigid body integrators described in Section 3 to general multi-body systems. We first focus on the standard continuous setting and then develop the corresponding geometric structure-preserving integrators.

5.1 The Continuous Setting

The configuration of a tree-topology multi-body system is defined as $q = (g, r) \in SE(3) \times \mathbb{R}^m$ with velocity given by $v = (\xi, \dot{r}) \in \mathbb{R}^{6+m}$, where $g \in SE(3)$ is the 4x4 pose matrix describing the base body orientation $R \in SO(3)$ and position $x \in \mathbb{R}^3$ according to

$$g = \left[\begin{array}{cc} R & x \\ 0_{1\times 3} & 1 \end{array} \right], \qquad g^{-1} = \left[\begin{array}{cc} R^T & -R^T x \\ \mathbf{0} & 1 \end{array} \right].$$

and where $\xi = (\omega, \mathsf{v}) \in \mathbb{R}^6$ defines its body-fixed angular velocity $\omega \in \mathbb{R}^3$ and linear velocity $\mathsf{v} \in \mathbb{R}^3$. The body-fixed velocity ξ is related to the configuration using the relationship [31, 21]

$$\dot{g} = g\hat{\xi},$$

where the operator $\hat{\cdot} : \mathbb{R}^6 \to \mathfrak{se}(3)$ turns velocities $\xi = (\mathsf{v}, \omega)$ into the 4x4 matrices

$$\hat{\xi} = \left[\begin{array}{cc} \hat{\omega} & \mathsf{v} \\ 0_{1\times 3} & 0 \end{array} \right]. \tag{43}$$

The Lagrangian of the system is defined by

$$L(g, r, \xi, \dot{r}) = \frac{1}{2}(\xi, \dot{r})^T \mathcal{M}(r)(\xi, \dot{r}) - V(g, r), \tag{44}$$

or more compactly as $L(q, v) = \frac{1}{2}v^T \mathcal{M}(r)v - V(q)$, where the mass matrix $\mathcal{M}$ is defined by (e.g. see [31, 34])

$$\mathcal{M}(r) = \left[\begin{array}{c|c} \mathbb{I}_0 + \sum_{i=1}^{n} A_i^T \mathbb{I}_i A_i & \sum_{i=1}^{n} A_i^T \mathbb{I}_i J_i \\ \hline \sum_{i=1}^{n} J_i^T \mathbb{I}_i A_i & \sum_{i=1}^{n} J_i^T \mathbb{I}_i J_i \end{array} \right] \tag{45}$$

where $\mathbb{I}_i$ is the 6x6 inertia matrix of body i and the adjoint notation $A_i \triangleq \mathrm{Ad}_{g_{0i}^{-1}(r)}$, and Jacobian $J_i \triangleq \sum_{j=1}^{n} [g_{0i}^{-1}(r)\partial_{r_j} g_{0i}(r)]^\vee$ were employed (the operator $\cdot^\vee$ is the inverse of the operator $\hat{\cdot}$ defined in (43)). Here we use the standard notation $g_{0i} : \mathbb{R}^m \to SE(3)$ to define the transformation between the base body (with index #0) and body #i (see e.g. [31]). The adjoint map Ad_g is defined by the 6x6 matrix

$$\mathrm{Ad}_g = \left[\begin{array}{cc} R & 0 \\ \hat{x}R & R \end{array} \right]. \tag{46}$$

13

Various efficient methods exist [30, 34] to compute the Jacobians and the mass matrix recursively exploiting the tree structure of the multi-body system. Finally, assume that the system is subject to generalized forces expressed through the known function $f(q, v, u)$. The variational principle used to obtain the dynamics is

$$\delta \int L(g, r, \xi, \dot{r})dt + \int \langle f(g, r, \xi, \dot{r}, u), (\eta, \delta r) \rangle = 0, \tag{47}$$

where the *left-trivialized* variation $\eta \in \mathbb{R}^6$ is defined by $\eta(t) = (g(t)^{-1}\delta g(t))^{\vee}$. The resulting equations of motion are obtained by taking variations $(\delta g, \delta r)$ and $(\delta \xi, \delta r)$ subject to the constraint (see e.g. [21])

$$\delta \xi = \dot{\eta} + \text{ad}_\xi \, \eta,$$

where the adjoint operator ad_ξ is defined by the 6x6 matrix

$$\text{ad}_\xi = \left[\begin{array}{cc} \hat{\omega} & 0 \\ \hat{v} & \hat{\omega} \end{array} \right].$$

This variational constraint stems from the kinematic constraints $\xi = (g^{-1}\dot{g})^{\vee}$ between ξ and g.

Before stating the equations of motion it is necessary to define a procedure for differentiating functions on the Lie group $SE(3)$. This will be accomplished by applying a trivialized gradient as opposed to the standard gradient on $\mathbb{R}^n$ as follows.

Definition 5.1. *The* left-trivialized gradient $g^*\nabla_g V(g) \in \mathbb{R}^6$ *of a function* $V : SE(3) \to \mathbb{R}$,

$$g^*\nabla V(g) = \nabla_\xi \Big|_{\xi=0} V(g \exp(\xi))$$

or in coordinates using the standard basis $\{e_1, \ldots, e_6\}$ *of* $\mathbb{R}^6$ *by*

$$g^*\nabla V(g) = \left[\frac{\partial V}{\partial s}\Big|_{s=0} (x \exp(se_1)), \; \cdots, \; \frac{\partial V}{\partial s}\Big|_{s=0} (x \exp(se_6)) \right]^T.$$

Continuous Equations of Motion. Employing the momenta $\mu = \partial_\xi L$ and $p = \partial_{\dot{r}} L$ the resulting dynamics can be expressed as:

$$\left[\begin{array}{c} \xi \\ \dot{r} \end{array} \right] = M(r)^{-1} \left[\begin{array}{c} \mu \\ p \end{array} \right] \tag{48}$$

$$\left[\begin{array}{c} \dot{\mu} \\ \dot{p} \end{array} \right] = \left[\begin{array}{c} (ad_\xi)^T \mu \\ \frac{1}{2}(I_n \otimes v^T)\nabla M(r)v \end{array} \right] - \left[\begin{array}{c} g^*\nabla_g V \\ \nabla_r V \end{array} \right] + f(q, v, u), \tag{49}$$

The system evolution is then fully determined by adding the reconstruction equations

$$\dot{g} = g\hat{\xi}$$

which corresponds to setting $\dot{R} = R\omega$ and $\dot{x} = Rv$. Note that equations (48) and (49) can be regarded as an extension of the standard Hamiltonian form of the equations of motion (see e.g. [29]) to floating-base systems. In order to derive the corresponding geometric integrator we next specify a methodology for performing discrete-time updates on Lie groups, such as $SE(3)$, without resorting to local coordinates.

5.2   Trajectory Discretization on Lie groups

A trajectory is represented numerically using a set of $N + 1$ equally spaced in time points denoted $g_{0:N} := \{g_0, ..., g_N\}$, where $g_k \approx g(kh) \in G$ and $h = T/N$ denotes the time-step. The section between each pair of points g_k and g_{k+1} is interpolated by a short curve that must lie on the manifold (Fig. 3). The simplest way to construct such a curve is through a map $\tau : \mathfrak{g} \to G$ and velocity vector $\xi_k \in \mathfrak{g}$ such that $\xi_k = \tau^{-1}(g_k^{-1}g_{k+1})/h$. Here $\mathfrak{g} \equiv T_e G$ denotes the Lie algebra of G. The map is defined as follows.

Definition 5.2. The *retraction map* $\tau : \mathfrak{g} \to G$ is a C^2-diffeomorphism around the origin such that $\tau(0) = e$. It is used to express small discrete changes in the group configuration through unique Lie algebra elements. For our purposes, we consider maps such that $\tau(\xi) = \exp(\xi) + O(\|\xi\|^3)$.

Thus, if ξ_k were regarded as an average velocity between g_k and g_{k+1} then τ is an approximation (to at least second-order) to the integral flow of the dynamics. The important point, from a numerical point of view, is that the difference $g_k^{-1}g_{k+1} \in G$, which is an element of a nonlinear space, can now be represented uniquely by the vector ξ_k in order to enable unconstrained optimization in the linear space $\mathfrak{g}$ for optimal control purposes.
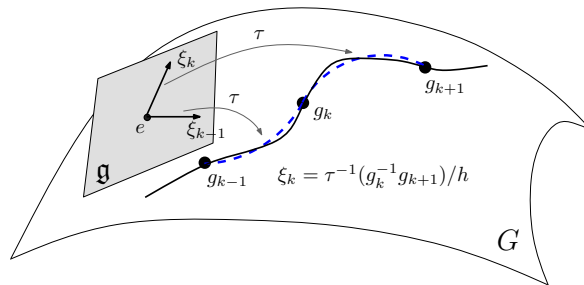

Figure 3: A trajectory (solid) on the Lie group G discretized using a sequence of arcs (dashed) represented by Lie algebra vectors $\xi_k \in \mathfrak{g}$ through the retraction map τ [27].

Next, we define the following operators related to τ.

Definition 5.3. [28, 23] Given a map $\tau : \mathfrak{g} \to G$, its *right-trivialized tangent* $\mathrm{d}\tau_\xi : \mathfrak{g} \to \mathfrak{g}$ and its *inverse* $\mathrm{d}\tau_\xi^{-1} : \mathfrak{g} \to \mathfrak{g}$ are such that, for a some $g = \tau(\xi) \in G$ and $\eta \in \mathfrak{g}$, the following holds

$$\partial_\xi \tau(\xi) \cdot \eta = \mathrm{d}\tau_\xi \cdot \eta \cdot \tau(\xi), \tag{50}$$

$$\partial_\xi \tau^{-1}(g) \cdot \eta = \mathrm{d}\tau_\xi^{-1} \cdot (\eta \cdot \tau(-\xi)). \tag{51}$$

Note that it can be shown by differentiating the expression $\tau^{-1}(\tau(\xi)) = \xi$ that

$$d\tau_\xi^{-1} \cdot d\tau_\xi \cdot \eta = \eta,$$

to confirm that these linear maps are indeed the inverse of each other.

Retraction Map (τ) Choices

a) The *exponential map*
$\exp : \mathfrak{g} \to G$, defined by $\exp(\xi) = \gamma(1)$, with $\gamma : \mathbb{R} \to G$ is the integral curve through the identity of the vector field associated with $\xi \in \mathfrak{g}$ (hence, with $\dot\gamma(0) = \xi$). The right-trivialized derivative of the map exp and its inverse are defined as

$$\mathrm{dexp}_x y = \sum_{j=0}^\infty \frac{1}{(j+1)!} \mathrm{ad}_x^j y, \tag{52a}$$

$$\mathrm{dexp}_x^{-1} y = \sum_{j=0}^\infty \frac{B_j}{j!} \mathrm{ad}_x^j y, \tag{52b}$$

where B_j are the Bernoulli numbers. Typically, these expressions are truncated in order to achieve a desired order of accuracy. The first few Bernoulli numbers are $B_0 = 1$, $B_1 = -1/2$, $B_2 = 1/6$, $B_3 = 0$ (see [15]).

b) The *Cayley map* $\mathrm{cay} : \mathfrak{g} \to G$ is defined by $\mathrm{cay}(\xi) = (\mathrm{I} - \xi/2)^{-1}(\mathrm{I} + \xi/2)$ and is valid for a general class for quadratic groups that include the groups of interest in the paper. Based on this simple form, the derivative maps become ([15], §IV.8.3)

$$\mathrm{dcay}_x y = \left(e - \frac{x}{2}\right)^{-1} y \left(e + \frac{x}{2}\right)^{-1}, \tag{53a}$$

$$\mathrm{dcay}_x^{-1} y = \left(e - \frac{x}{2}\right) y \left(e + \frac{x}{2}\right). \tag{53b}$$

The third choice is to use canonical coordinates of the second kind (ccsk) [15] which are based on the exponential map and are not considered in this paper. In our implementation we employ the Cayley map the details for which are given next.

The Cayley map for rigid body transformations

The algorithms developed in this paper are based on the the Cayley map for $SE(3)$ since it is often a better alternative to the exponential for computational efficiency and ease of implementation that does not require special numerical handling at the origin. With a slight abuse of notation, i.e. assuming the identification $\mathfrak{g} \sim \mathbb{R}^6$, the Cayley map $\tau : \mathbb{R}^6 \to SE(3)$ is defined as (see [27])

$$\tau(\xi) = \left[\begin{array}{cc} I_3 + \frac{4}{4+\|\omega\|^2}\left(\widehat{\omega} + \frac{\widehat{\omega}^2}{2}\right) & \frac{2}{4+\|\omega\|^2}\left(2I_3 + \widehat{\omega}\right)v \\ 0 & 1 \end{array} \right], \tag{54}$$

while the matrix representation of the right-trivialized tangent inverse $\mathrm{d}\tau_\xi^{-1} : \mathbb{R}^6 \to \mathbb{R}^6$ becomes

$$[\mathrm{d}\tau_\xi^{-1}] = \left[\begin{array}{cc} I_3 - \frac{1}{2}\widehat{\omega} + \frac{1}{4}\omega\omega^T & 0_3 \\ -\frac{1}{2}\left(I_3 - \frac{1}{2}\widehat{\omega}\right)\widehat{v} & I_3 - \frac{1}{2}\widehat{\omega} \end{array} \right]. \tag{55}$$

5.3 Discrete Variational Formulation

With a discrete trajectory in place we follow the approach taken in [35, 25, 26] in order to construct a structure-preserving (i.e. group, momentum, and symplectic) integrator of the dynamics. We make a simple extension to include potential and control forces through a trapezoidal quadrature approximation. In particular, the action in (1) is approximated along each discrete segment between points (g_k, r_k) and (g_{k+1}, r_{k+1}) through

$$\int_{kh}^{(k+1)h} L(g, r, \xi, \dot{r})\, \mathrm{d}t \approx h L_d(g_k, g_{k+1}, r_k, r_{k+1}), \tag{56a}$$

$$\int_{kh}^{(k+1)h} \langle f, (\eta, \delta r)\rangle \mathrm{d}t \approx \left[\langle f_d^-(g_k, g_{k+1}, r_k, r_{k+1}), (\eta_k, \delta r_k)\rangle + \langle f_d^-(g_k, g_{k+1}, r_k, r_{k+1}), (\eta_{k+1}, \delta r_{k+1})\rangle\right]. \tag{56b}$$

where the discrete variation $\eta_k \in \mathbb{R}^6$ is defined by $\eta_k = (g_k^{-1}\delta g_k)^\vee$. The discrete Lagrangian and forces are defined by

$$L_d(g_k, g_{k+1}, r_k, r_{k+1}) = \frac{h}{2}\left[L(g_k, r_k, \xi_{k+1}, \Delta r_{k+1}) + L(g_{k+1}, r_{k+1}, \xi_{k+1}, \Delta r_{k+1})\right], \tag{57}$$

$$f_d^-(g_k, g_{k+1}, r_k, r_{k+1}, u_k, u_{k+1}) = \frac{h}{2}S(h\xi_{k+1})^T f(g_k, r_k, \xi_{k+1}, \Delta r_{k+1}, u_k), \tag{58}$$

$$f_d^+(g_k, g_{k+1}, r_k, r_{k+1}, u_k, u_{k+1}) = \frac{h}{2}S(-h\xi_{k+1})^T f(g_{k+1}, r_{k+1}, \xi_{k+1}, \Delta r_{k+1}, u_{k+1}), \tag{59}$$

where the discrete velocities $\xi_k \in \mathbb{R}^6$ and $\Delta r_k \in \mathbb{R}^m$ are defined by

$$\xi_k \triangleq \tau^{-1}(g_{k-1}^{-1}g_k)/h, \qquad \Delta r_k \triangleq (r_k - r_{k-1})/h.$$

The matrix $S(\xi)$ is defined by

$$S(\xi) = \left[\begin{array}{cc} \mathrm{d}\tau_\xi^{-1} & 0 \\ 0 & I_m \end{array} \right] \tag{60}$$

and is interpreted as a Jacobian (or push-forward) map which transforms average vectors along a segment generated by ξ to vectors defined at the beginning of the segment [2, 9]. The map τ and its tangent $\mathrm{d}\tau^{-1}$ are defined in (54) and (55) and implemented through simple matrix-vector products. Finally, note that we have the following variational constraint which may be obtained through differentiation and application of (51),

$$\delta\xi_k = \delta\tau^{-1}(g_{k-1}^{-1}g_k)/h = [-\mathrm{d}\tau_{h\xi_k}^{-1}\eta_{k-1} + \mathrm{d}\tau_{-h\xi_k}^{-1}\eta_k]/h, \tag{61}$$

which serves as the basis for applying the variational principle on Lie groups and also the reason why $S(\xi)$ appears in (58) and (59).

Discrete Equations of Motion. The resulting geometric integrator from applying the principle (1) using the discrete Lagrangian (57) and forces (58) and (59) subject to the constraint (61) is:

$$g_{k+1} = g_k \tau(h\xi_{k+1}) \tag{62}$$

$$r_{k+1} = r_k + h\Delta r_{k+1} \tag{63}$$

$$\frac{1}{2}S(h\xi_{k+1})^T[M(r_k) + M(r_k + h\Delta r_{k+1})]v_{k+1} - \frac{1}{2}S(-h\xi_k)^T[M(r_{k-1}) + M(r_k)]v_k =$$

$$\frac{h}{4}\begin{bmatrix} 0 \\ (I_n \otimes v_{k+1}^T)\nabla\mathcal{M}(r_k)v_{k+1} + (I_n \otimes v_k^T)\nabla\mathcal{M}(r_k)v_k \end{bmatrix} - h\begin{bmatrix} g^*\nabla_g V(q_k) \\ \nabla_r V(q_k) \end{bmatrix} \tag{64}$$

$$+ \frac{h}{2}\left[S(h\xi_{k+1})^T f(q_k, v_{k+1}, u_k) + S(-h\xi_k)^T f(q_k, v_k, u_k) \right].$$

Applying Newton's Algorithm. The discrete equations of motion (62)–(64) are used to update the current state $(q_k, v_k) = (g_k, r_k, \xi_k, \Delta r_k)$ to obtain the next state $(q_{k+1}, v_{k+1}) = (g_{k+1}, r_{k+1}, \xi_{k+1}, \Delta r_{k+1})$. This is accomplished by first solving the dynamics (64) using a root-finding algorithm such as Newton's method in terms of the unknowns $v_{k+1} = (\xi_{k+1}, \Delta r_{k+1})$ which are then used in the explicit equations (62)–(63) to obtain the next configuration $q_{k+1} = (g_{k+1}, r_{k+1})$.

5.4 Preservation Properties

One of the main benefits of employing the variational numerical framework lies in its preservation properties, summarized as follows.

Symplectic structure. The discrete flow (64) preserves the discrete symplectic form, expressed in coordinates as

$$\omega_L = \frac{\partial^2 L_d(q_k, q_{k+1})}{\partial q_k^i \partial q_{k+1}^j}\, \mathrm{d}q_k^i \wedge \mathrm{d}q_{k+1}^j,$$

where $\wedge$ is the standard wedge product between differential forms [21]. The symplectic form is physically related to the phase space structure. Its preservation during integration, for instance, signifies that a volume of initial conditions would not be spuriously inflated or deflated due to numerical approximations. Volume preservation means that the orbits of the dynamics will have a predictable character and no artificial damping normally employed by Runge-Kutta methods is needed to stabilize the system [1].

Momentum Conservation. The discrete dynamics (64) also exactly preserves any Lagrangian symmetries. In particular, assume that there is a group G whose action on Q leaves the Lagrangian invariant in the sense that

$$L(q, v) = L(\exp(s\rho)q, v),$$

which implies that

$$L_d(q_k, q_{k+1}) = L_d(\exp(s\rho)q_k, \exp(s\rho)q_{k+1}),$$

for some $\rho \in \mathfrak{g}$, where $\mathfrak{g}$ is the Lie algebra of G, and s is a scalar. In this case the momentum map $J(q_k, q_{k+1}) \cdot \rho = D_1 L_d(q_k, q_{k+1}) \cdot \rho_Q(q_k)$ is preserved [1] where ρ_Q is the infinitesimal generator of the group [21]. Practically speaking, whenever the continuous system preserves momentum, so does the discrete. Any change in the momentum then exactly reflects the work done by non-conservative forces. Such a momentum-symplectic scheme also exhibits long-term stable energy behavior close to the true system energy [1].

For instance, assume that the Lagrangian of a multi-body system is invariant with respect to spatial rotations and translations and that there are no external or control forces acting on the base body. In this case we have $G = SE(3)$ and the momentum map

$$J(q_k, q_{k+1}) = \begin{bmatrix} \mathrm{Ad}_{g_k^{-1}}^T & 0_m \end{bmatrix} \frac{1}{2}S(h\xi_{k+1})^T[M(r_k) + M(r_k + h\Delta r_{k+1})]v_{k+1} \tag{65}$$

is exactly preserved by the integrator.
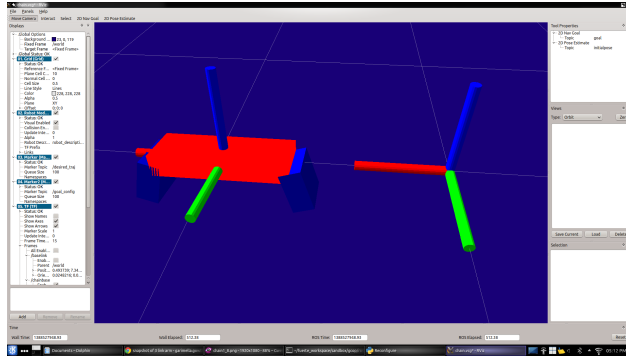
ROS-based multi-body system simulation user interface
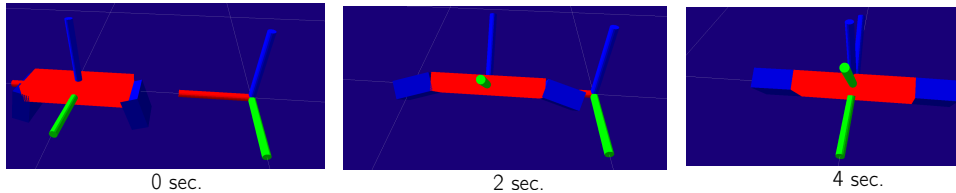

0 sec.   2 sec.   4 sec.

Figure 4: A simple three-link chain with hinge joints simulated by the symplectic integrator and visualized using the Robot Operating System (ROS) user interface.

Order of Accuracy. The order of accuracy of the dynamics update depends on the accuracy of the Lagrangian approximation. Since the trapezoidal approximations (56a) and (56b) are employed then it can be shown (see [1]) that the discrete equations (64) are at least *second order accurate*. The trapezoidal rule was chosen since it provides one of the simplest second-order scheme. Higher-order methods by proper choice of the Lagrangian, termed symplectic Runge-Kutta (see [15, 26, 23]), are possible but not considered in this work.

Group structure. Finally, the group structure is exactly preserved since each configuration g_k is reconstructed from the previous pose g_{k-1} and the discrete velocity ξ_k using the map τ which by definition maps to the group $SE(3)$. This avoids issues with dissipation and numerical drift associated with reprojection used for instance in explicit methods based on matrix orthogonality constraints or quaternions.

5.5 Numerical Example

These numerical properties are illustrated with a simple multibody system consisting of three bodies in 3-D arranged in a chain connected with hinge joints (Figure 4). The system is free-floating with the central body taken as the base body with index #0. No control or external forces are applied in order to verify the integrator momentum conservation properties. Figure 5 illustrates the resulting time-histories of the velocities ω and v, joint angles r, momentum components J (corresponding to the vector (65)) and position x. The true trajectory was constructed using an Euler step with step-size $h = 0.001$ sec. while the step-size for both the symplectic method (symp) and Euler method (euler) were $h = 0.1$ sec. The figures show that momentum is exactly preserved by the symplectic method. The purpose of this study is not to preform detailed comparisons but only to validate the basic numerical features of the method. The main point is that these results motivate a further study to extend the coordinate-based convergence conditions (41) to Lie group methods for mechanical systems.

6 Conclusion

This paper considered numerical properties of geometric integrators for multi-body systems related to the choice of time-step h. Such methods exhibit favorable numerical stability and accuracy but require
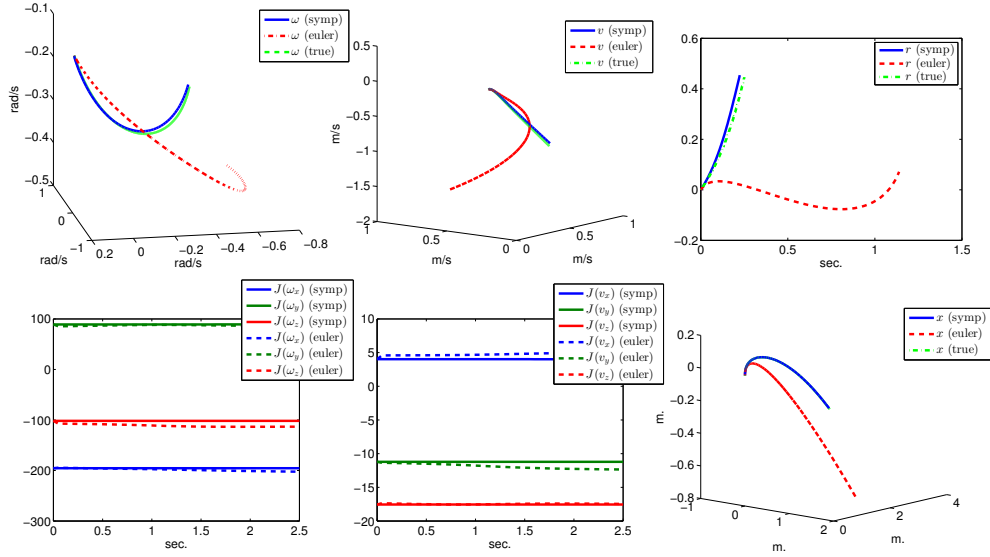
18

Figure 5: The proposed symplectic integrators preserve the momentum map J and remain highly accurate even at large time-step (in this example $h = 0.1$ sec). The key issue which remains to be answered is how high can h be chosen while retaining the solvability of the implicit time-stepping.

the solution of a potentially complex system of nonlinear equations. We showed that the solvability of this system can be guaranteed by ensuring that h is chosen below an upper bound $\bar{h}$ determined from the dynamical model parameters and previous state of the system. The availability of such a bound a priori is important since it could enable predictable computation times for real-time integration or optimal control purposes. For instance, a number of previously developed optimal control methods based on geometric integrators [36, 37, 38, 39, 27] could benefit from a formal method for establishing the resolution of discrete trajectories used for optimization.

Further work is necessary to provide guidelines for the practical application of the proposed bounds. While the derived upper limits for a single rigid body are simple and straightforward to use (i.e. they depend on the inertia condition number and norm of velocity), the situation with general multibody systems is more complex. We showed that second-order geometric integrators in either generalized coordinates and or using $SE(3)$ matrices directly can be used as a basis for provably solvable time-stepping. Further study is necessary to establish a procedure for computing the dynamical model functions $\ell_0, \ldots, \ell_6$ based on the type of system under consideration.

While we considered variational integrators the proposed methodology could be extended to other energy-consistent low-order methods such as the discrete null space method [40]. A more challenging but equally important direction is to establish time-stepping bounds for more general systems involving intermittent contacts [41, 42, 43, 44, 45, 46, 47].

References

[1] J. Marsden and M. West, "Discrete mechanics and variational integrators," *Acta Numerica*, vol. 10, pp. 357–514, 2001.

[2] M. Kobilarov, K. Crane, and M. Desbrun, "Lie group integrators for animation and control of vehicles," *ACM Trans. Graph.*, vol. 28, no. 2, pp. 1–14, 2009.

[3] L. Kharevych, Weiwei, Y. Tong, E. Kanso, J. Marsden, P. Schroder, and M. Desbrun, "Geometric, variational integrators for computer animation," in *Eurographics/ACM SIGGRAPH Symposium on Computer Animation*, 2006, pp. 1–9.

[4] E. Barth and B. Leimkuhler, "Symplectic methods for conservative multibody systems," *Fields Institute Communications*, vol. 10, pp. 25–43, 1993.

19

[5] S. Reich, "Symplectic integrators for systems of rigid bodies," *Integration Algorithms and Classical Mechanics, volume 10 of Fields Institute Communications. AMS*, vol. 10, p. 383, 1996.

[6] L. Jay, "Symplectic partitioned rungekutta methods for constrained hamiltonian systems," *SIAM Journal on Numerical Analysis*, vol. 33, no. 1, pp. 368–387, 1996. [Online]. Available: http://epubs.siam.org/doi/abs/10.1137/0733019

[7] S. Leyendecker, J. E. Marsden, and M. Ortiz, "Variational integrators for constrained dynamical systems," *Zeitschrift fr Angewandte Mathematik und Mechanik*, vol. 88, no. 9, pp. 677–708, 2008.

[8] E. Johnson and T. Murphey, "Scalable variational integrators for constrained mechanical systems in generalized coordinates," *IEEE Transactions on Robotics*, vol. 25, no. 6, pp. 1249 – 1261, 2009.

[9] M. Kobilarov, J. E. Marsden, and G. S. Sukhatme, "Geometric discretization of nonholonomic systems with symmetries," *AIMS Journal on Discrete and Continuous Dynamical Systems - Series S (DCDS-S)*, vol. 3, no. 1, pp. 61 – 84, 2010.

[10] N. S. Peter Betsch, Christian Hesch and S. Uhlar, "Variational integrators and energy-momentum schemes for flexible multibody dynamics," *J. Comput. Nonlinear Dynam*, vol. 5, no. 3, 2010.

[11] E. Barth, B. Leimkuhler, and S. Reich, "A semi-explicit, variable-stepsize, time-reversible integrator for constrained dynamics," *SIAM J. Sci. Comput*, 1997.

[12] K. Modin, D. Fritzson, C. Fuhrer, and G. Soderlind, "A new class of variable step-size methods for multibody dynamics," in *MULTIBODY DYNAMICS 2005, ECCOMAS Thematic Conference*, 2005.

[13] K. Modin and C. Fü hrer, "Time-step adaptivity in variational integrators with application to contact problems," *ZAMM*, vol. 86, no. 10, pp. 785–794, 2006.

[14] R. Holsapple, R. Iyer, and D. Doman, "Variable step-size selection methods for implicit integration schemes for odes," *Int. J. Numer. Anal. Mod.*, no. 4, pp. 210–240, 2007.

[15] E. Hairer, C. Lubich, and G. Wanner, *Geometric Numerical Integration*, ser. Springer Series in Computational Mathematics. Springer-Verlag, 2006, no. 31.

[16] F. Park, J. Bobrow, and S. Ploen, "A lie group formulation of robot dynamics," *The International Journal of Robotics Research*, vol. 14, no. 6, pp. 609–618, 1995. [Online]. Available: http://ijr.sagepub.com/content/14/6/609.abstract

[17] A. Mueller and P. Maisser, "A lie-group formulation of kinematics and dynamics of constrained mbs and its application to analytical mechanics," *Multibody System Dynamics*, vol. 9, pp. 311–352, 2003.

[18] J. Park and W.-K. Chung, "Geometric integration on euclidean group with application to articulated multibody systems," *Robotics, IEEE Transactions on*, vol. 21, no. 5, pp. 850 – 863, oct. 2005.

[19] A. Muller and Z. Terze, "Differential-geometric modelling and dynamic simulation of multibody systems," *Journal for Theory and Application in Mechanical Engineering*, vol. 51, no. 6, 2009.

[20] C. Lanczos, *Variational Principles of Mechanics*. University of Toronto Press, 1949.

[21] J. E. Marsden and T. S. Ratiu, *Introduction to Mechanics and Symmetry*. Springer, 1999.

[22] P. Krysl and L. Endres, "Explicit newmark/verlet algorithm for time integration of the rotational dynamics of rigid bodies," *International Journal for Numerical Methods in Engineering*, 2005.

[23] N. Bou-Rabee and J. Marsden, "Hamilton-pontryagin integrators on Lie groups," *Foundations of Computational Mathematics*, vol. 9, pp. 197–219, 2009.

[24] E. Celledoni and B. Owren, "Lie group methods for rigid body dynamics and time integration on manifolds," *Comput. meth. in Appl. Mech. and Eng.*, vol. 19, no. 3,4, pp. 421–438, 2003.

[25] J. E. Marsden, S. Pekarsky, and S. Shkoller, "Discrete euler-poincare and Lie-poisson equations," *Nonlinearity*, vol. 12, p. 16471662, 1999.

[26] M. Leok, "Foundations of computational geometric mechanics," Ph.D. dissertation, California Institute of Technology, 2004.

[27] M. Kobilarov and J. Marsden, "Discrete geometric optimal control on Lie groups," *IEEE Transactions on Robotics*, vol. 27(4), pp. 641–655, 2011.

[28] A. Iserles, H. Z. Munthe-Kaas, S. P. Nørsett, and A. Zanna, "Lie group methods," *Acta Numerica*, vol. 9, pp. 215–365, 2000.

[29] F. Lewis, D. Dawson, and C. Abdallah, *Robot Manipulator Control: Theory and Practice*, ser. Automation and Control Engineering. Taylor & Francis, 2003. [Online]. Available: http://books.google.com/books?id=8002tURlPP4C

[30] R. Featherstone, *Rigid Body Dynamics Algorithms*. Springer, 2008.

[31] R. M. Murray, Z. Li, and S. S. Sastry, *A Mathematical Introduction to Robotic Manipulation*. CRC, 1994.

[32] P. Deuflhard, *Newton methods for nonlinear problems : affine invariance and adaptive algorithms*, ser. Springer series in computational mathematics. Berlin, Heidelberg, New York: Springer, 2004, autre tirage : 2006. [Online]. Available: http://opac.inria.fr/record=b1101121

[33] W. B. Gragg and R. A. Tapia, "Optimal error bounds for the newton-kantorovich theorem," *SIAM Journal on Numerical Analysis*, vol. 11, no. 1, pp. pp. 10–13, 1974. [Online]. Available: http://www.jstor.org/stable/2156425

[34] A. Jain, *Robot and Multibody Dynamics: Analysis and Algorithms*. Springer, 2011.

[35] A. I. Bobenko and Y. B. Suris, "Discrete lagrangian reduction, discrete euler-poincare equations, and semidirect products," *Letters in Mathematical Physics*, vol. 49, p. 79, 1999.

[36] M. de Leon, D. M. de Diego, and A. Santamaria Merino, "Geometric numerical integration of non-holonomic systems and optimal control problems," *European Journal of Control*, vol. 10, pp. 520–526, 2004.

[37] T. Lee, M. Leok, and N. McClamroch, "Lie group variational integrators for the full body problem in orbital mechanics," *Celestial Mechanics and Dynamical Astronomy*, vol. 98, no. 2, pp. 121–144, 2007.

[38] A. M. Bloch, I. I. Hussein, M. Leok, and A. K. Sanyal, "Geometric structure-preserving optimal control of a rigid body," *Journal of Dynamical and Control Systems*, vol. 15, no. 3, pp. 307–330, 2009.

[39] S. Leyendecker, S. Ober-Blbaum, J. E. Marsden, and M. Ortiz, "Discrete mechanics and optimal control for constrained systems," *Optimal Control Applications and Methods*, vol. 31, no. 6, pp. 505–528, 2010. [Online]. Available: http://dx.doi.org/10.1002/oca.912

[40] P. Betsch and S. Leyendecker, "The discrete null space method for the energy consistent integration of constrained mechanical systems. part ii: multibody dynamics," *International Journal for Numerical Methods in Engineering*, vol. 67, no. 4, pp. 499–552, 2006. [Online]. Available: http://dx.doi.org/10.1002/nme.1639

[41] F. Pfeiffer and C. Glocker, *Multibody Dynamics with Unilateral Contacts*. Wiley Series in Nonlinear Science, 1996.

[42] M. Anitescu, "Optimization-based simulation of nonsmooth rigid multibody dynamics," *Mathematical Programming*, vol. 105, pp. 113–143, 2006. [Online]. Available: http://dx.doi.org/10.1007/s10107-005-0590-7

[43] F. A. Potra, M. Anitescu, B. Gavrea, and J. Trinkle, "A linearly implicit trapezoidal method for integrating stiff multibody dynamics with contact, joints, and friction," *International Journal for Numerical Methods in Engineering*, vol. 66, no. 7, pp. 1079–1124, 2006. [Online]. Available: http://dx.doi.org/10.1002/nme.1582

[44] C. Studer, *Numerics of Unilateral Contacts and Friction, Modeling and Numerical Time Integration in Non-Smooth Dynamics*. Springer, 2009.

[45] M. W. Koch and S. Leyendecker, "Optimal control of multibody dynamics with contact," *PAMM*, vol. 11, no. 1, pp. 51–52, 2011. [Online]. Available: http://dx.doi.org/10.1002/pamm.201110017

[46] A. Jain, C. Crean, C. Kuo, H. V. Bremen, and S. Myint, "Minimal coordinate formulation of contact dynamics in operational space," in *Robotics: Science and Systems*, 2012.

[47] N. Chakraborty, S. Berard, S. Akella, and J. Trinkle., "A geometrically implicit time-stepping method for multibody systems with intermittent contact," *International Journal of Robotics Research*, vol. 32, no. tbd, p. tbd, 2013.